

Research



Cite this article: Maity B, Banerjee S, Senapati A, Chattopadhyay J. 2023 Quantifying optimal resource allocation strategies for controlling epidemics. *J. R. Soc. Interface* **20**: 20230036.
<https://doi.org/10.1098/rsif.2023.0036>

Received: 29 January 2023
 Accepted: 25 April 2023

Subject Category:
 Life Sciences—Mathematics interface

Subject Areas:
 biomathematics, computational biology

Keywords:
 resource allocation, disease outbreak, intervention strategy, production function

Authors for correspondence:
 Swarnendu Banerjee
 e-mail: swarnendubanerjee92@gmail.com
 Abhishek Senapati
 e-mail: abhishekiz4u04@gmail.com

Electronic supplementary material is available online at <https://doi.org/10.6084/m9.figshare.c.6631156>.

Quantifying optimal resource allocation strategies for controlling epidemics

Biplab Maity¹, Swarnendu Banerjee^{1,2}, Abhishek Senapati^{1,3} and Joydev Chattopadhyay¹

¹Agricultural and Ecological Research Unit, Indian Statistical Institute, 203, B. T. Road, Kolkata 700108, India

²Copernicus Institute of Sustainable Development, Utrecht University, PO Box 80115, Utrecht 3508 TC, The Netherlands

³Center for Advanced Systems Understanding (CASUS), Untermarkt 20, Goerlitz 02826, Germany

BM, 0009-0001-5318-0506; SB, 0000-0003-2308-2136; AS, 0000-0003-1572-2658

Frequent emergence of communicable diseases is a major concern worldwide. Lack of sufficient resources to mitigate the disease burden makes the situation even more challenging for lower-income countries. Hence, strategy development for disease eradication and optimal management of the social and economic burden has garnered a lot of attention in recent years. In this context, we quantify the optimal fraction of resources that can be allocated to two major intervention measures, namely reduction of disease transmission and improvement of healthcare infrastructure. Our results demonstrate that the effectiveness of each of the interventions has a significant impact on the optimal resource allocation in both long-term disease dynamics and outbreak scenarios. The optimal allocation strategy for long-term dynamics exhibits non-monotonic behaviour with respect to the effectiveness of interventions, which differs from the more intuitive strategy recommended in the case of outbreaks. Further, our results indicate that the relationship between investment in interventions and the corresponding increase in patient recovery rate or decrease in disease transmission rate plays a decisive role in determining optimal strategies. Intervention programmes with decreasing returns promote the necessity for resource sharing. Our study provides fundamental insights into determining the best response strategy when controlling epidemics in resource-constrained situations.

1. Introduction

Infectious diseases like influenza, severe acute respiratory syndrome (SARS), Ebola and, most recently, COVID-19 spread throughout a population within a short time, making it a cause of utmost concern for human society [1–7]. The lack of appropriate health policies, protective medical equipment such as disposable gloves and surgical masks, poorly developed infrastructure and shortage of medical personnel make it even more challenging for low-income countries to mitigate the health crisis during an ongoing outbreak [8–10]. This can be well understood, for instance, by considering the severe impact of Ebola on West African countries such as Nigeria, Liberia and Sierra Leone, where there was an estimated shortage of 7.2 million doctors and health workers [11,12]. Furthermore, estimates also indicate that nearly 79% of the total available hospital beds would be required for patients with influenza in lower-income countries, with an incidence rate of 35%. In countries such as Bangladesh and Nepal, even with an incidence rate of 15%, the demand for hospital beds exceeds the capacity [9]. Due to resource limitations, governments are often required to make difficult decisions when allocating a fixed budget among different healthcare and disease reduction programmes [13]. Therefore, the optimal allocation of resources is a necessary component of public health responses to control the spread of infectious diseases.

A simplistic way to look at control of infectious disease outbreaks is either by prevention of transmission through non-pharmaceutical interventions (NPIs), such as social distancing, personal hygiene, contact tracing and early detection, or by improvement of recovery rate through better medical treatment. The World Health Organization [14,15] and governmental health agencies in many countries publish disease prevention protocols to fight disease outbreaks [16–18]. These are often promoted using social media advertisements and educational programmes to increase awareness about the prevention of a particular disease. Implementation of various preventive measures helps to diminish the contact rate between infected and susceptible individuals, thereby reducing the transmission rate. Although NPIs are likely to be effective at an early stage of a disease outbreak, often it is not possible to keep the disease transmission under control, for instance, when there is a sharp rise in the number of new infections. Additionally, there are difficulties in implementing control measures such as lockdowns or travel restrictions due to huge economic and societal costs, mainly in developing countries [19,20]. In such cases, it is important to ramp up hospital infrastructure and consequently prioritize the quality of treatment which would influence the recovery of infected individuals, thus reducing the potential impact of an epidemic [21–23]. Such measures would include increasing the number of hospital beds [24], setting up temporary medical units, training programmes for healthcare personnel [9] and procuring more medical equipment and medicines.

Designing efficient and feasible control strategies that maintain a balance between the implementation of pharmaceutical interventions and NPIs in resource-constrained situations is essential to reduce the potential impact of disease burden. However, in both cases, the effectiveness of the interventions plays a key role in determining the success of the implemented strategies. One intervention measure is said to be more effective than another if a better recovery rate or a reduced transmission rate is achieved at the expense of the same resources. For instance, to mitigate Ebola and SARS, symptom monitoring programmes become a more effective measure than quarantine, whereas the benefit of quarantine over symptom monitoring has been observed for diseases like influenza and smallpox [25]. Also, face covering appears to be a more effective way to prevent COVID-19 than quarantine and social distancing measures [26]. On the other hand, treatment protocols using drugs like remdesivir were shown to be more effective than hydroxychloroquine during the early stages of the COVID-19 pandemic [27,28]. Furthermore, the relationship between invested resources and the corresponding outcome of an intervention programme, also known as the production function, plays a decisive role in determining optimal strategies [29]. Since the outcome of an intervention depends on its effectiveness, the latter influences the steepness of a particular type of production function. Hence, it is important to design resource allocation policies that take into account the effectiveness of available intervention programmes and their corresponding production functions.

To analyse a range of possible scenarios under specific epidemic situations, mathematical modelling has been used as an important and reliable tool to guide policy-making and implementation of different intervention programmes. In this regard, several attempts have been made that

investigated different aspects of optimal resource allocation strategies [30–39]. Many of these studies have focused on resource allocation to only prevention programmes related to vaccination [30] or transmission reductions, such as face mask distribution [34] and testing [37,38]. Few studies have also considered resource allocation between two different strategies, such as vaccination and isolation, but did not take into account any explicit trade-off between them [33,39]. Thus these studies lack in providing a theoretical framework to study optimal resource allocation between two broad classes of intervention strategies—transmission reduction and improving healthcare infrastructure, where there can be trade-offs between the two. While a recent study examined the allocation of resources between prevention and treatment, the role of the effectiveness of the former was not explored [31]. Moreover, the study was based on HIV transmission, and hence did not consider a recovered class, which might be relevant for other diseases. For the same reason, the optimal strategy was determined by considering only specific types of production functions.

In this study, we fill this gap and attempt to provide a general understanding of how limited resources may be optimally allocated between transmission-reducing and recovery-improvement programmes, taking into account the effectiveness of both types of interventions. Using a simple susceptible–infected–recovered (SIR) model, we quantify the optimal fraction of resources required to minimize the impact of disease burden under both long-term disease dynamics and outbreaks. We study the roles of different types of production functions and explore how the optimal strategy varies with the effectiveness of the intervention measures. Furthermore, since there are often delays in reporting new infections, and proper knowledge about a disease is not typically available at early stages, we also quantify the optimal fraction of resources in the presence of delays in implementing interventions.

2. Methods

2.1. Model

We consider the well-known compartmental SIR model [40,41] to represent the disease dynamics. At time t , the fractions of susceptible, infected and recovered population are denoted by $S(t)$, $I(t)$ and $R(t)$, respectively, which satisfies the constraint $S(t) + I(t) + R(t) = 1$. The rate of change of the fraction of people in each compartment can be described as follows:

$$\left. \begin{aligned} \frac{dS}{dt} &= \mu - \beta_0 SI - \mu S, \\ \frac{dI}{dt} &= \beta_0 SI - \gamma_0 I - \mu I \\ \text{and} \quad \frac{dR}{dt} &= \gamma_0 I - \mu R. \end{aligned} \right\} \quad (2.1)$$

Here, β_0 is the disease transmission rate, μ is the birth and death rate, and γ_0 is the recovery rate. The basic reproduction number, \mathcal{R}_0 , defined as the average number of secondary cases appearing from an average primary case in an entirely susceptible population, can be obtained as $\mathcal{R}_0 = \beta_0 / (\gamma_0 + \mu)$.

We introduce control strategies using available resources among competing prevention and treatment programmes. Here, one can think of the available resources as the total financial budget for government investment in healthcare. A natural consequence of the allocation of resources is an alteration in disease

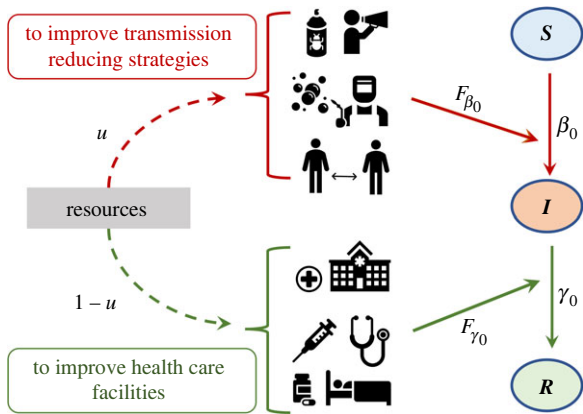


Figure 1. Optimal resource allocation. The total resources available for disease control are allocated to two broad classes of interventions, namely, transmission-reducing interventions such as awareness programmes, personal hygiene, social distancing etc. and intervention programmes that would improve healthcare facilities, which in turn shorten the infectious period and speed up the process of recovery. Here, u is the fraction of the total available resources allocated to transmission-reducing interventions, and the remaining $(1 - u)$ fraction is allocated to improve healthcare facilities. This process of resource allocation is incorporated into the classical SIR model by introducing the production functions F_{β_0} and F_{γ_0} , which reflect the effect of resource allocation on the transmission rate (β_0) and recovery rate (γ_0), respectively.

transmission rates and recovery rates that affect epidemic outcomes. Here, a fraction u of total available resources is allocated for implementing transmission-reducing strategies, and the remaining fraction, i.e. $(1 - u)$ is devoted to improving healthcare infrastructure (see the schematic in figure 1). The fact that the total available resources to reduce disease burden are fixed signifies a trade-off between allocations to the two types of competing intervention programmes.

The relationship between the invested resources and outcomes of intervention programmes, described by the production function, determines the true impact of public health interventions. We denote $F_{\beta_0}(u)$ and $F_{\gamma_0}(1 - u)$ as the production functions associated with transmission-reducing and recovery-improvement programmes, respectively. To reflect the effect of resource implementation, we replace β_0 and γ_0 in model (2.1) with $F_{\beta_0}(u)$ and $F_{\gamma_0}(1 - u)$, respectively (see the schematic in figure 1). Thus, the model with interventions can be written as

$$\left. \begin{aligned} \frac{dS}{dt} &= \mu - F_{\beta_0}(u)SI - \mu S, \\ \frac{dI}{dt} &= F_{\beta_0}(u)SI - F_{\gamma_0}(1 - u)I - \mu I \\ \text{and} \quad \frac{dR}{dt} &= F_{\gamma_0}(1 - u)I - \mu R. \end{aligned} \right\} \quad (2.2)$$

Now, production functions, F_{β_0} and F_{γ_0} can be broadly categorized into three types, as described below. For each incremental investment in the intervention programmes, the associated production function, $F_{\beta_0}(F_{\gamma_0})$, yields decreasing, constant or increasing returns to scale if the corresponding reduction (improvement) in the transmission (recovery) rate is increasingly smaller, remains constant or increasingly larger, respectively (figure 2) [32,35]. For the sake of comparison, we assume that three types of returns considered for $F_{\beta_0}(F_{\gamma_0})$ are equivalent to each other at the two extreme cases, i.e. when $u = 0$ or $u = 1$ (figure 2). Furthermore, it is important to note that there is always a limited realizable benefit from an intervention programme, regardless of investment [29,35]. This implies that there always will be a lower limit to the reducible

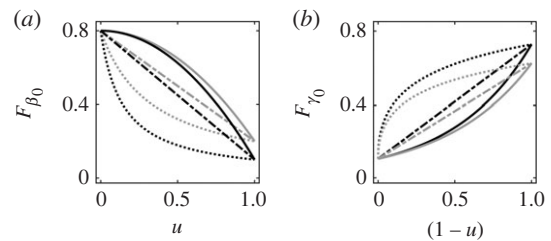


Figure 2. Different types of production functions: (a) $F_{\beta_0}(u)$ and (b) $F_{\gamma_0}(1 - u)$ corresponding to transmission-reducing and recovery-improvement interventions, respectively. Here, the solid, dashed and dotted lines represent the increasing, constant and decreasing returns to scale, respectively. In (a), (b), the production functions with lower and higher effectiveness parameters are presented in grey and black colour, respectively. For the specific forms of F_{β_0} and F_{γ_0} , see electronic supplementary material, S53.

transmission rate and an upper limit to the achievable recovery rate. However, these limits depend on the effectiveness of the intervention strategies. For the same resources, a more effective intervention measure implies a greater reduction (increase) in the transmission (recovery) rate (figure 2).

We consider the production functions $F_{\beta_0}(u) = \beta_0 / (1 + \beta_e u)$ and $F_{\gamma_0}(1 - u) = \gamma_0(1 + \gamma_e(1 - u))$, where the parameter β_e indicates the effectiveness of transmission-reducing interventions and the parameter γ_e denotes the effectiveness of recovery-improving interventions. Here, F_{β_0} and F_{γ_0} have decreasing and constant returns to scale, respectively. The motivation for such consideration comes from several theoretical as well as empirical studies on resource allocation for HIV prevention programmes, such as needle exchange [42] and condom distribution [31,43], and treatment programmes such as antiretroviral therapy [31,44] and methadone maintenance [45,46]. However, our consideration of the effectiveness of recovery-improving interventions is different from that of the treatment effectiveness in [31] as the latter does not increase the recovery rate but reduces the infectivity of susceptibles after treatment. Note that if both β_e and γ_e are set to zero, model (2.2) will be reduced to the original model (2.1). Now in the presence of control strategy, we define control reproduction number \mathcal{R}_0^c as

$$\begin{aligned} \mathcal{R}_0^c &= \frac{F_{\beta_0}(u)}{F_{\gamma_0}(1 - u) + \mu} \\ &= \frac{\beta_0}{(1 + \beta_e u)(\gamma_0(1 + \gamma_e(1 - u)) + \mu)}. \end{aligned}$$

While the F_{β_0} and F_{γ_0} defined above receive the majority of our attention, other types of production functions are also considered to address potential alternative socio-economic scenarios. We use the phrases *improving healthcare facilities* and *improving recovery*, and also *transmission-reducing* and *prevention* programmes interchangeably throughout the paper.

2.2. Model parametrization and simulations

We take the numerical value of the model parameters like birth/death rate, disease transmission rate and recovery rate, from previous studies. The parameters related to effectiveness are varied in our study. The initial conditions S_0 and I_0 are chosen based on the assumption that almost everyone in the population is initially susceptible. All simulations in this study are performed using parameters in table 1 unless specified otherwise.

Here, two different measures of disease burden, one corresponding to the long-term endemic dynamics and another corresponding to the short-term outbreak dynamics, are used as objective functions. To obtain the optimal fraction of resources numerically, first, the values of u are spaced linearly between 0

Table 1. Description of parameters for the model (2.1).

parameters	description	value	references
μ	natural birth and death rate of human	$\frac{1}{70} \text{ yr}^{-1}$	[47,48]
β_0	transmission rate	0.8 d^{-1}	[47]
γ_0	recovery rate	0.1 d^{-1}	[47,49]
β_e	effectiveness of transmission-reducing interventions	varied	—
γ_e	effectiveness of recovery-improving interventions	varied	—
S_0, I_0	initial proportion of susceptible, infected individuals	0.999, 0.001	assumed

and 1 with a suitable step length. Next, we integrate the model (2.2) numerically using *ode45* in Matlab (Mathworks, R2018a) and calculate the objective functions for each value of u . Finally, we select the optimal value of u for which the objective functions return the minimum value.

3. Results

We investigate the problem of optimal resource allocation in two scenarios: (i) long-term or endemic disease dynamics and (ii) dynamics of disease during an outbreak. In the first scenario, demographic factors are considered, i.e. the birth and death rates are non-zero, while in the second scenario, we ignore birth and natural death rates to capture the short-term disease dynamics.

In the following subsections, we first describe the results for both the long-term and outbreak scenarios obtained from our model using the specific forms of F_{β_0} and F_{γ_0} described in §2. Subsequently, we describe the results by considering three types of returns to scale for each F_{β_0} and F_{γ_0} and all their possible combinations.

3.1. Resource allocation for long-term dynamics of the disease

To control long-term disease persistence, we take the proportion of infected individuals at equilibrium (I^*) as the objective function, which is to be minimized in the presence of allocated resources. From the resource-implemented model (2.2), we can find the proportion of susceptible (S^*) and infected (I^*) individuals at equilibrium analytically using nullclines as

$$S^* = \begin{cases} 1/\mathcal{R}_0^c & \text{if } \mathcal{R}_0^c > 1 \\ 1 & \text{if } \mathcal{R}_0^c \leq 1 \end{cases}$$

and

$$I^* = \begin{cases} \frac{\mu}{F_{\beta_0}}(\mathcal{R}_0^c - 1) & \text{if } \mathcal{R}_0^c > 1 \\ 0 & \text{if } \mathcal{R}_0^c \leq 1. \end{cases} \quad (3.1)$$

When $\mathcal{R}_0^c > 1$, the endemic equilibrium is locally asymptotically stable while the disease-free equilibrium exists but is unstable. The equilibria merge when $\mathcal{R}_0^c = 1$ and only a stable disease-free equilibrium exists when $\mathcal{R}_0^c < 1$. This implies that the number of infected individuals asymptotically approaches a non-zero endemic level when $\mathcal{R}_0^c > 1$ and zero when $\mathcal{R}_0^c \leq 1$.

To find the optimal fraction of resources in the former case, i.e. when $\mathcal{R}_0^c > 1$, I^* is differentiated with respect to u and set equal to zero. Then, simple algebraic manipulation allows us to solve for u , which we denote as u_1

$$u_1 = \frac{\beta_e(\gamma_0 + \gamma_0\gamma_e + \mu) - \sqrt{\beta_0\beta_e\gamma_0\gamma_e}}{\beta_e\gamma_0\gamma_e}. \quad (3.2)$$

It is important to note that the fraction of resources allocated must be constrained between 0 and 1. Taking this into account, it can be shown that when $\mathcal{R}_0^c \leq 1$, the optimal fraction of resources can lie anywhere in a certain interval $[u_1, u_2] \subseteq [0, 1]$ (electronic supplementary material, §S1). Hence, we can define the optimal fraction of resources to prevent transmission in the case of long-term disease dynamics, u_{long}^* , as follows:

$$u_{\text{long}}^* = \begin{cases} 0 & \text{if } u_1 \leq 0 \\ u_1 & \text{if } 0 < u_1 < 1 \\ 1 & \text{if } u_1 \geq 1 \end{cases} \left. \vphantom{u_{\text{long}}^*} \right\} \mathcal{R}_0^c > 1 \quad (3.3)$$

$$\left. \vphantom{u_{\text{long}}^*} \right\} [u_1, u_2] \subseteq [0, 1] \mathcal{R}_0^c \leq 1.$$

Now, we explore the behaviour of u_{long}^* with respect to the effectiveness of intervention programmes β_e and γ_e when $\mathcal{R}_0^c > 1$. Here, $\lim_{\beta_e \rightarrow 0} u_{\text{long}}^* = 0$ (because $\lim_{\beta_e \rightarrow 0} u_1 \rightarrow -\infty$) indicates that when β_e is too low, the optimal strategy is to allocate the entire resources to recovery-improvement programmes. This holds true until a threshold, $\beta_e^l = \beta_0\gamma_0\gamma_e/(\gamma_0 + \gamma_0\gamma_e + \mu)^2$ above which u_{long}^* increases with β_e implying the need to allocate increasing fractions of resources to prevention programmes (figure 3a). It is interesting to note that β_e^l is non-monotonic in γ_e . As a result, we can see that the threshold for $\gamma_e = 1$ shifts towards the right from the threshold for $\gamma_e = 0.5$, but for higher values of γ_e ($\gamma_e = 2, 5$), the threshold shifts toward the left (figure 3a).

Similarly, $\lim_{\gamma_e \rightarrow 0} u_{\text{long}}^* = 1$ (because $\lim_{\gamma_e \rightarrow 0} u_1 \rightarrow +\infty$) implies that when γ_e is too low, the optimal strategy is to devote entire resources to transmission-reducing programmes. Again, this holds true only until a threshold $\gamma_e^l = \beta_e(\gamma_0 + \mu)^2/(\beta_0\gamma_0)$ above which u_{long}^* starts to decrease with γ_e . This trend persists until a second threshold, $\tilde{\gamma}_e = 4\beta_e(\gamma_0 + \mu)^2/(\beta_0\gamma_0)$ after which the optimal strategy is to allocate decreasing fractions of resources toward treatment programmes (see figure 3b). Furthermore, the sensitivity of our findings to the baseline model parameters (β_0 , γ_0 and μ) is discussed in electronic supplementary material, §S1, and shown in figure S1.

To better understand the role of the effectiveness parameters in optimal resource allocation, the two-parameter

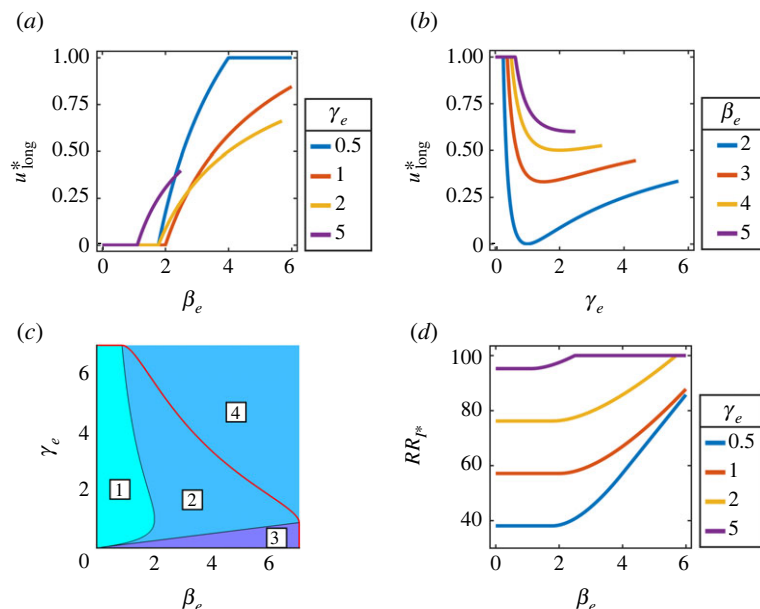


Figure 3. Role of effectiveness parameters in determining the optimal fraction of allocated resources to control disease dynamics in a long-term scenario. The optimal fraction of resources (a) with respect to β_e , (b) with respect to γ_e , and (c) when both effectiveness parameters, β_e and γ_e , are varied simultaneously. The red line in (c) indicates $\mathcal{R}_0^c = 1$. Here, unique u_{long}^* is associated with $\mathcal{R}_0^c > 1$ (displayed as [1], [2] and [3]), whereas non-unique u_{long}^* is associated with $\mathcal{R}_0^c \leq 1$ (displayed as [4]). [1] represents the region where $u_{\text{long}}^* = 0$; i.e. allocating entire resources towards the recovery-improvement programmes is the optimal strategy. [3] represents the region where the allocation of entire resources toward the transmission-reducing programmes is the optimal strategy (i.e. $u_{\text{long}}^* = 1$). [2] and [4] represent the regions for resource-sharing between the two types of intervention programmes. Here, u_{long}^* has unique values between 0 and 1 in [2]. Also, u_{long}^* lies within certain intervals in [4]. (d) Relative reduction (RR_{I^*}) of I^* with respect to β_e for different values of γ_e .

space ($\beta_e - \gamma_e$) can be divided into four regions (figure 3c). We vary β_e and γ_e till the values such that only one type of intervention itself cannot achieve an asymptotically stable disease-free state. Here [1], [2] and [3] are associated with the locally asymptotically stable endemic state of the prevalence (where $\mathcal{R}_0^c > 1$). In [1] and [3], the optimal strategy is to allocate entire resources for recovery-improvement (i.e. $u_{\text{long}}^* = 0$) and transmission-reducing programmes (i.e. $u_{\text{long}}^* = 1$), respectively. In [2], there are unique optimal strategies between 0 and 1 determined by the effectiveness parameters, which signifies the need for allocating resources to both prevention and treatment. The resulting control reproduction number can then be expressed as

$$\mathcal{R}_0^{\text{long}} = \frac{\sqrt{\beta_0 \beta_e \gamma_0 \gamma_e}}{\beta_e (\gamma_0 + \mu) + \gamma_0 \gamma_e (1 + \beta_e) - \sqrt{\beta_0 \beta_e \gamma_0 \gamma_e}}. \quad (3.4)$$

Here, the lines separating [2] from [1] and [3] are formed by the threshold values β_e^l and γ_e^l mentioned above. [4] corresponds to $\mathcal{R}_0^c \leq 1$ where u_{long}^* is not unique but can vary between certain ranges (see §S1 and figure S2 in electronic supplementary material). With increasing β_e and γ_e , the range of values of u_{long}^* in [4] increases, signifying greater flexibility in choosing optimal strategy (electronic supplementary material, figure S2). The line $\mathcal{R}_0^c = 1$ denotes the borderline between [4] and [2] (red line in figure 3c). It can also be interpreted as the line of critical thresholds $\beta_e^{\text{crit}}(\gamma_e)$ or $\gamma_e^{\text{crit}}(\beta_e)$, i.e. the least values of β_e and γ_e which will lead to stable disease-free state asymptotically under optimal resource allocation. Overall, we see that the optimal strategy changes from allocating resources in a single intervention in [1] and [3] to dividing resources between both interventions in [2] and [4] under different values of effectiveness parameters.

We now quantify the relative impact of resource allocation on disease dynamics. For this, we consider an uncontrolled epidemic (i.e. when both β_e and γ_e are zero) as the baseline scenario. We then calculate the percentage of relative reduction (RR_{I^*}) of the objective function I^* by varying the effectiveness parameters in the presence of resource allocation (figure 3d). For small values of γ_e , such as $\gamma_e = 0.5, 1, 2$, if we vary β_e in the interval $0 \leq \beta_e \lesssim 2$, the relative reduction in I^* stays almost the same at approximately 38%, 57% and 76%, respectively (figure 3d). Since, for these γ_e values within $0 \leq \beta_e \lesssim 2$, $u_{\text{long}}^* = 0$ is found to be optimal (figure 3a), therefore we do not observe any role of β_e in the reduction of I^* . However, if we further increase β_e ($2 \leq \beta_e \leq 6$), we observe a gradual increase in RR_{I^*} (figure 3d). This is because u_{long}^* is non-zero in this case, and both β_e and γ_e have non-zero contributions. If γ_e is fixed at a relatively higher value, such as $\gamma_e = 5$, RR_{I^*} can reach about 95% (figure 3d).

3.2. Resource allocation for an outbreak scenario

For an outbreak scenario, we ignore natural birth and death in our model; i.e. we fix $\mu = 0$ in our model (2.2). In this case, the control reproduction number can be expressed as $\mathcal{R}_0^{\text{out}} = \beta_0 / (\gamma_0(1 + \beta_e u)(1 + \gamma_e(1 - u)))$. The basic characteristics of an outbreak can be inferred from the sign of $dI/dt|_{t=0}$ or equivalently $1 - S_0 \mathcal{R}_0^{\text{out}}$. When $S_0 \mathcal{R}_0^{\text{out}} > 1$, the number of infected individuals initially increases until it reaches its maximum, and subsequently decays. When $S_0 \mathcal{R}_0^{\text{out}} = 1$, the outbreak is initially in a stationary state and subsequently decays. For $S_0 \mathcal{R}_0^{\text{out}} < 1$, the outbreak is initially in a decaying state and remains to decay for all subsequent time. The epidemic peak is defined as the maximum number of infected individuals attained during an disease outbreak. Since the peak is a primary indicator of the severity

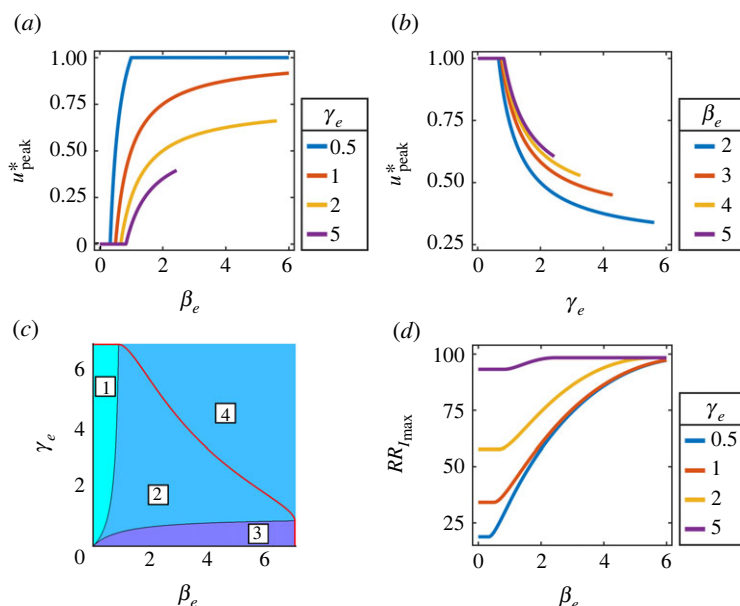


Figure 4. Role of effectiveness parameters in determining the optimal fraction of allocated resources to control disease in an outbreak scenario. The optimal fraction of resources (a) with respect to β_e , (b) with respect to γ_e , and (c) when both effectiveness parameters, β_e and γ_e , are varied simultaneously. The red line indicates $S_0 \mathcal{R}_0^{\text{out}} = 1$. Unique u_{peak}^* corresponds to the initial growth of the outbreak size (i.e. $S_0 \mathcal{R}_0^{\text{out}} > 1$, displayed as [1], [2] and [3]), whereas non-unique u_{peak}^* is associated with the initial decay of the outbreak size (i.e. $S_0 \mathcal{R}_0^{\text{out}} < 1$, displayed as [4]). [1] represents the region where $u_{\text{peak}}^* = 0$, i.e. allocating entire resources towards the recovery-improvement programmes is the optimal strategy. [3] represents the region where the allocation of entire resources to transmission-reducing programmes is the optimal strategy (i.e. $u_{\text{peak}}^* = 1$). [2] and [4] represent the regions for resource-sharing between the two types of intervention programmes. Here, u_{peak}^* has unique values between 0 and 1 in [2]. Also, u_{peak}^* lies within certain intervals in [4]. (d) Relative reduction ($RR_{I_{\text{max}}}$) of I_{max} with respect to β_e for different values of γ_e .

of an outbreak, lowering it is one of the primary goals for reducing the burden of outbreaks.

For this purpose, we analytically derive the epidemic peak (I_{max}) (electronic supplementary material, §S2), which can be expressed as follows:

$$I_{\text{max}} = \begin{cases} S_0 + I_0 - \frac{(\ln(S_0 \mathcal{R}_0^{\text{out}}) + 1)}{\mathcal{R}_0^{\text{out}}} & \text{if } S_0 \mathcal{R}_0^{\text{out}} > 1 \\ I_0 & \text{if } S_0 \mathcal{R}_0^{\text{out}} \leq 1. \end{cases} \quad (3.5)$$

In the case of initially growing outbreaks (i.e. $S_0 \mathcal{R}_0^{\text{out}} > 1$), the optimal fraction of resources can be obtained by differentiating I_{max} with respect to u , setting it equal to zero, and solving algebraically (electronic supplementary material, §S2)

$$u_p = \frac{1}{2} \left(1 - \frac{1}{\beta_e} + \frac{1}{\gamma_e} \right). \quad (3.6)$$

Furthermore, when the outbreak is initially in a stationary or decaying state, one can solve the inequality $S_0 \mathcal{R}_0^{\text{out}} \leq 1$ for u to obtain the optimal fraction of resources in the form of an interval $[u_{p_1}, u_{p_2}]$ (electronic supplementary material, §S2). As the fraction of allocated resources must be constrained between 0 and 1, a new quantity, u_{peak}^* is defined as the optimal fraction of resources invested in transmission-reducing programmes such that

$$u_{\text{peak}}^* = \begin{cases} 0 & \text{if } u_p \leq 0 \\ u_p & \text{if } 0 < u_p < 1 \\ 1 & \text{if } u_p \geq 1 \end{cases} \left\{ S_0 \mathcal{R}_0^{\text{out}} > 1 \right. \quad (3.7)$$

$$\left. \left[u_{p_1}, u_{p_2} \right] \subseteq [0, 1] \right\} S_0 \mathcal{R}_0^{\text{out}} \leq 1.$$

It can be observed from equation (3.6) for u_p that u_{peak}^* depends only on the effectiveness of intervention programmes β_e, γ_e when $S_0 \mathcal{R}_0^{\text{out}} > 1$ and is independent of the transmission rate and recovery rate β_0, γ_0 . Similar to the long-term scenario, we explore the behaviour of u_{peak}^* with respect to β_e and γ_e .

Here, $\lim_{\beta_e \rightarrow 0} u_{\text{peak}}^* = 0$ (because $\lim_{\beta_e \rightarrow 0} u_p \rightarrow -\infty$) indicates that when β_e is too low, the optimal strategy is to allocate the entirety of resources to recovery-improvement programmes. This holds true until a certain threshold $\beta_e^p = \gamma_e / (1 + \gamma_e)$ after which u_{peak}^* increases with β_e (figure 4a). Similarly, $\lim_{\gamma_e \rightarrow 0} u_{\text{peak}}^* = 1$ (because $\lim_{\gamma_e \rightarrow 0} u_p \rightarrow +\infty$) implies that when γ_e is too low, the optimal strategy is to devote the entirety of resources to transmission-reducing programmes. Again, this holds true only until a threshold $\gamma_e^p = \beta_e / (1 + \beta_e)$ above which u_{peak}^* starts to decrease with γ_e (figure 4b). Notably, in this case, the monotonic behaviour of u_{peak}^* with respect to β_e and γ_e indicates that the optimal control strategy is to allocate more resources to intervention programmes with better effectiveness (figure 4a,b).

Parameter space ($\beta_e - \gamma_e$) can be divided into four regions based on the optimal strategy (figure 4c). As in figure 3c, β_e and γ_e are varied till the values such that resource allocation to only one type of intervention cannot satisfy the condition for the initial decay state of an outbreak. Here [1], [2] and [3] correspond to $S_0 \mathcal{R}_0^{\text{out}} > 1$, where the optimal fraction of resources towards transmission prevention, u_{peak}^* , is given by 0, u_p and 1, respectively. In [2], where u_p is the unique optimal strategy, the control reproduction number for the outbreak scenario is given by

$$\mathcal{R}_0^{\text{peak}} = \frac{4\beta_0\beta_e\gamma_e}{\gamma_0(\beta_e\gamma_e + \beta_e + \gamma_e)^2}. \quad (3.8)$$

The curves that separate [1] and [3] from [2] correspond to threshold values β_e^p and γ_e^p respectively. In contrast to figure 3c, [1] and [3] are symmetric about the line $\beta_e = \gamma_e$. This can be explained by the fact that both $\beta_e^p(\gamma_e)$ and $\gamma_e^p(\beta_e)$ satisfy the same underlying function. Further, it is interesting to note that $u_p(\beta_e, \gamma_e) = 1 - u_p(\gamma_e, \beta_e)$. This implies that if the effectiveness of prevention and treatment programmes is reversed in the case

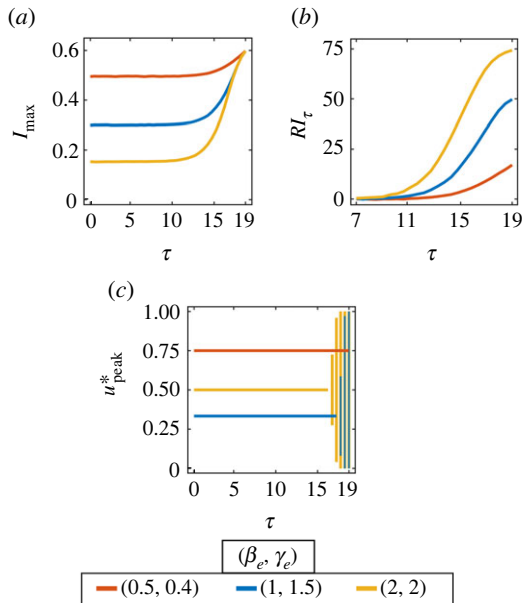


Figure 5. Effect of delay (τ) in implementing interventions during a disease outbreak for different combinations of β_e and γ_e . (a) The peak of infection (I_{\max}) as a function of τ . (b) Percentage of the relative increase in I_{\max} compared with the immediate intervention (i.e. $\tau=0$) with respect to τ . (c) The optimal fraction of resources (u_{peak}^*) aimed at minimizing the peak of infection as a function of τ . The vertical lines represent the range of possible values of u_{peak}^* when non-unique.

of certain diseases, then the optimal strategy corresponds to the reversal of resource allocation. For optimally used resources with increased effectiveness, the outbreak is unable to initially grow (i.e. $S_0\mathcal{R}_0^{\text{out}} \leq 1$), which is represented by [4]. Within [4], u_{peak}^* is non-unique and varies between certain ranges (electronic supplementary material, S2). The line $S_0\mathcal{R}_0^{\text{out}} = 1$ (red line) separates [4] from [2] in figure 4c. It can also be interpreted as the line of critical values $\beta_e^{\text{crit}}(\gamma_e)$ or $\gamma_e^{\text{crit}}(\beta_e)$, i.e. the lowest values of β_e and γ_e which are sufficient to prevent the outbreak from growing initially under optimal resource allocation.

With respect to the baseline scenario of uncontrolled epidemics (i.e. $\beta_e = \gamma_e = 0$), we calculate the percentage of the relative reduction ($RR_{I_{\max}}$) of I_{\max} by varying the effectiveness parameters in the presence of optimal resources (see figure 4d). For lower values of β_e , when $u_{\text{peak}}^* = 0$ is optimal (figure 4a), we see from figure 4d that approximately 18%, 34%, 57% and 93% reductions can be achieved for $\gamma_e = 0.5, 1, 2$ and 5, respectively. A further increase in β_e leads to a gradual increase in $RR_{I_{\max}}$.

3.2.1. Impact of delays in resource implementation

In reality, it is reasonable to expect a delay between the implementation of intervention measures and the onset of an outbreak due to inappropriate information about it at an early stage. To explore the impact of such delays during outbreaks, we calculate the peak of infection (I_{\max}) when the control measures are implemented τ days after the onset of the outbreak (figure 5a). We also calculate the percentage of relative increase (RI_τ) in the peak of infection for each delay time, τ , in comparison with the immediate implementation ($\tau=0$) (figure 5b). Finally, we calculate the corresponding optimal fraction of resources (u_{peak}^*) as a function of the delay time, τ , for different values of the effectiveness parameters in figure 5c. In our model, for an uncontrolled

epidemic (i.e. $\beta_e = \gamma_e = 0$), the infection curve reaches its peak at approximately $t = 19$. Since we are interested in peak minimization (lowering the curve of infection), we vary the implementation delay parameter (τ) from days $t = 0$ to $t = 19$.

For lower values of both effectiveness parameters β_e and γ_e (for instance, $\beta_e = 0.5$ and $\gamma_e = 0.4$), the peak of infection (I_{\max}) remains almost the same until day $\tau = 12$ (figure 5a, red curve). This means that both interventions with lower effectiveness allow a delay of up to 12 days in allocating resources without any significant consequences in terms of the peak of infection. However, if the allocation of resources is further delayed, a gradual increase in the peak of infection can be observed. We find that after a delay of 12 days, RI_τ increases gradually and reaches approximately 17% at $\tau = 19$ (figure 5b, red curve) for the lower effectiveness parameters. On the other hand, for higher values of both effectiveness parameters (for instance, $\beta_e = 2$ and $\gamma_e = 2$), if the implementation is delayed by more than 7 days, a larger increase in RI_τ (approx. 74% at $\tau = 19$; figure 5a,b, yellow curve) is observed compared with the lower effectiveness case. This is because interventions with higher effectiveness are capable of greater reductions in the peak of infection, and delays in implementing these interventions lead to a significant relative increase. It should also be noted that for lower values of the effectiveness parameters ($\beta_e = 0.5$ and $\gamma_e = 0.4$), the optimal fraction of resources (u_{peak}^*) remains unchanged with respect to delay (figure 5c, red curve). This is because u_{peak}^* depends only on β_e and γ_e (see equation (3.7)). Additionally, for lower values of these effectiveness parameters, the condition $S_\tau\mathcal{R}_0^{\text{out}} > 1$ is satisfied for all τ resulting in a unique optimal value (where S_τ denotes the proportion of susceptible individuals for the uncontrolled epidemic at $t = \tau$ day after the onset of the outbreak). For higher values of β_e and γ_e , u_{peak}^* behaves in a slightly different manner. Similar to the above-mentioned case, u_{peak}^* remains the same and takes a unique value until a threshold of τ is reached, where the quantity, $S_\tau\mathcal{R}_0^{\text{out}}$ becomes less than or equal to 1 (as the susceptible population depletes over time). Consequently, u_{peak}^* becomes non-unique and can take a range of possible values from an interval (see figure 5c, the blue and yellow curves).

3.3. Dependence of resource allocation on production functions

To study the robustness of our results, we choose a different F_{β_0} with decreasing returns, given as $F_{\beta_0} = \beta_0 e^{-u \ln(1+\beta)}$ (solid line in figure 6a). A similar exponential function has been used to estimate production functions for HIV prevention programmes [31,43]. For extreme values of u , the new F_{β_0} is equivalent to that assumed in the previous sections (figure 6a). As we want to keep the returns-to-scale type the same for a better comparison, and because F_{γ_0} exhibits constant returns to scale, it is kept unchanged. This implies that \mathcal{R}_0^c , evaluated at the extreme values of u , is the same as in §3.1. Consequently, in the long-term scenario, the line $\mathcal{R}_0^c = 1$ intersects β_e and γ_e axes at the same values as in figure 3c, thereby facilitating comparison. For the outbreak scenario, similar arguments hold for the line, $S_0\mathcal{R}_0^{\text{out}} = 1$.

We calculate optimal strategies for both long-term and outbreak scenarios for different effectiveness parameters in figure 6b,c and compare [1]–[4] with those in figures 3c and 4c. For the long-term case, the non-monotonic behaviour of β_e^l is retained, suggesting that this property might be

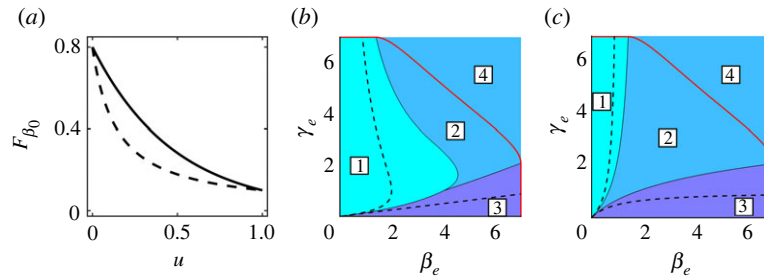


Figure 6. Comparison of optimal strategies under two different transmission-reducing production functions with decreasing returns to scale: $F_{\beta_0} = \beta_0 e^{-u \ln(1+\beta_e)}$ (black solid lines) and $F_{\beta_0} = \beta_0 / (1 + \beta_e u)$ (dashed lines). Production functions are shown in (a). Role of effectiveness parameters in the optimal fraction of allocated resources is demonstrated for the long-term in (b) and outbreak scenarios in (c). An increase in [1] and [3] is observed compared with the original form in figures 3c and 4c. Here, the red lines $\mathcal{R}_0^c = 1$ and $S_0 \mathcal{R}_0^{\text{out}} = 1$ in (b) and (c), respectively, are shown only for $F_{\beta_0} = \beta_0 e^{-u \ln(1+\beta_e)}$.

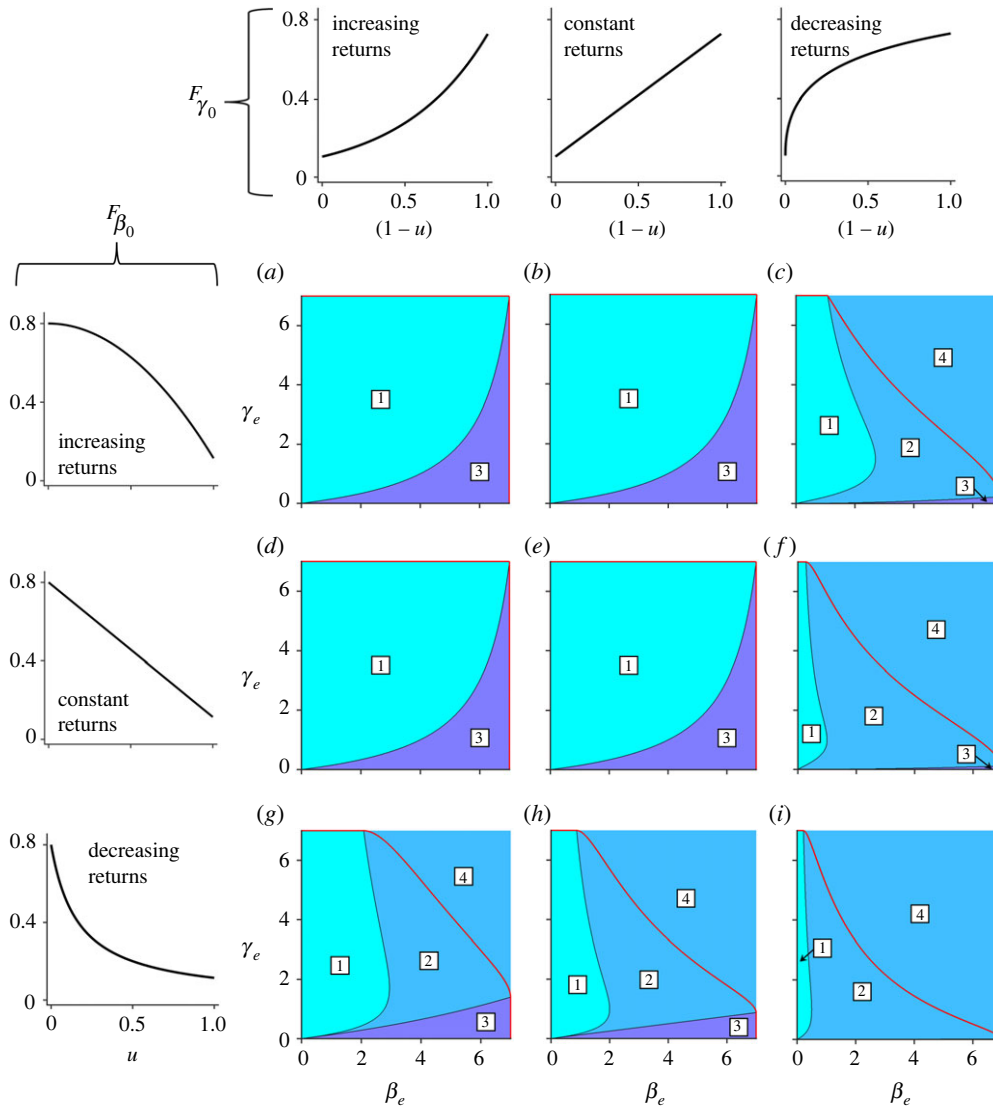


Figure 7. Comparison of optimal strategies considering three types of returns to scale for both F_{β_0} and F_{γ_0} to explore the dependence of optimal resource allocation on production functions for disease control in a long-term scenario. The characteristics of u_{long}^* within [1], [2], [3] and [4] are the same as those shown in figure 3c. For the specific forms of F_{β_0} and F_{γ_0} , see electronic supplementary material, S53.

independent of the functional forms of F_{β_0} with decreasing returns to scale. By contrast, for the outbreak scenario, the symmetric nature of [1] and [3] about the line $\beta_e = \gamma_e$ is lost, which implies that it can only be true in the case of certain production functions. Further, in this case, there is an increase in the area occupied by [1] and [3]. This signifies a greater possibility that allocating resources to either prevention or treatment programmes is an optimal strategy.

Till now, we have only considered decreasing and constant returns to scale for transmission-reducing and recovery-improvement programmes, respectively. However, it is important to understand the results obtained above in the context of other return types for production functions. Hence, in this section, we consider each of $F_{\beta_0}(u)$ and $F_{\gamma_0}(1-u)$ with increasing, constant and decreasing returns to scale and compare the results among all their combinations (figures 7 and 8).

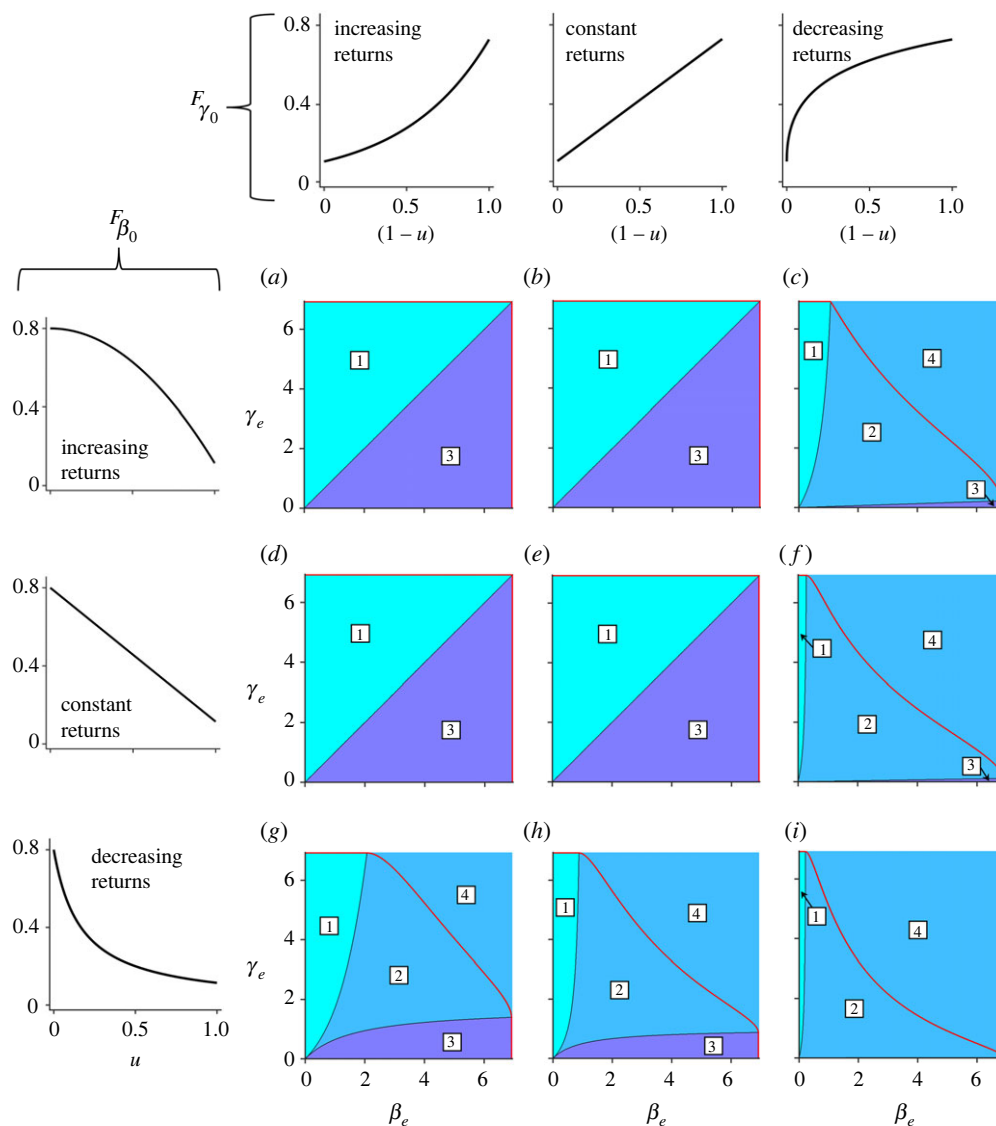


Figure 8. Comparison of optimal strategies considering three types of returns to scale for both F_{β_0} and F_{γ_0} to explore the dependence of optimal resource allocation on production functions for disease control in an outbreak scenario. The characteristics of u_{peak}^* within [1], [2], [3] and [4] are the same as those shown in figure 4c. For the specific forms of F_{β_0} and F_{γ_0} , see electronic supplementary material, S53.

For a more meaningful comparison between the results, we consider that the three types of returns to scale for F_{β_0} (the same for F_{γ_0}) are equivalent to each other when $u = 0$ or $u = 1$ (figure 2). The exact functional forms of $F_{\beta_0}(u)$ and $F_{\gamma_0}(1-u)$ are presented in electronic supplementary material, S53.

We observe that when F_{β_0} gives either increasing or constant returns to scale, and the same holds for F_{γ_0} , the optimal fraction of resources, u_{long}^* takes only extreme values (either 0 in [1] or 1 in [3]) (figure 7a,b,d,e). Interestingly, in these cases, u_{long}^* is independent of the functional forms of F_{β_0} and F_{γ_0} and has the same value for a particular β_e and γ_e (see electronic supplementary material, Prop. 1). On the other hand, when either or both F_{β_0} and F_{γ_0} have decreasing returns to scale, u_{long}^* also takes intermediate values between 0 and 1 (figure 7c,f–i). Furthermore, if F_{β_0} (F_{γ_0}) gives decreasing returns to scale, and F_{γ_0} (F_{β_0}) changes from increasing to decreasing returns to scale, we observe that regions [1] and [3] decrease (figure 7c,f,i and g,h,i). Moreover, decreasing returns to scale for both prevention and treatment programmes expand the parameter space in which resource sharing is optimal (figure 7i). These results indicate that decreasing returns from investments in intervention

programmes promote the necessity for resource sharing. Additionally, moving from increasing to decreasing returns to scale, the relatively lower effectiveness of interventions can be sufficient to obtain an asymptotically stable disease-free state; i.e. $\mathcal{R}_0^c < 1$. For instance, when $\beta_e = \gamma_e = 4$ in figure 7g, we have $\mathcal{R}_0^c > 1$ but the same conditions in figure 7i yield $\mathcal{R}_0^c < 1$. The intuition behind such an observation can be easily understood from the shapes of the curves F_{β_0} and F_{γ_0} . When compared with increasing or constant returns to scale, decreasing returns to scale for F_{β_0} and F_{γ_0} implies that relatively lower transmission and higher recovery rates can be achieved for the same investment (except at $u = 0, 1$). All of the results described above also hold true for the outbreak scenario (figure 8). It is important to mention that, for the long-term scenario, the non-monotonic behaviour of β_e^l with respect to γ_e is observed when at least one of F_{β_0} and F_{γ_0} has decreasing returns to scale (figure 7c,f–i).

4. Discussion

Designing effective intervention strategies is of the utmost importance in order to cope with disease outbreaks.

Particularly, in low-income countries, resource-constrained situations make it challenging for authorities to optimally allocate resources to mitigate epidemics. In this context, the resource allocation trade-off between the prevention of transmission and better medical treatment is significant, yet not well understood. To address this gap, we developed a simple model based on the SIR framework that considers production functions for intervention programmes and the associated effectiveness. The interplay between the effectiveness of the two major types of interventions and their implications for optimal resource allocation has been explored under two common epidemic scenarios: long-term and outbreak. While the former case concerns the minimization of the proportion of infected individuals at equilibrium, the primary objective of the latter is to minimize the peak of infection during a disease outbreak. For both scenarios, we observed the transitions from allocation of the entirety of resources to only one intervention type to optimal sharing of resources between both types of interventions under different effectiveness parameter settings (figures 3c and 4c). This behaviour is similar to the threshold-switching of the optimal isolation strategy observed in [33], and the transition of optimal testing from clinical to mixed strategies observed in [37].

In the long-term scenario, our results demonstrate that the prioritization of transmission-reducing interventions should increase monotonically with their effectiveness (figure 3a). This is suggestive of the fact that it is always advantageous to allocate maximum resources to disease prevention when highly effective preventive measures are available. Interestingly, the allocation of recovery-improving interventions does not always behave in a similar way. Owing to the constant influx of susceptible populations, there is an increased risk of new infections when prevention programmes are less effective. Thus, when treatment programmes are sufficiently effective (i.e. beyond a threshold), the optimal solution is to divert some resources to prioritize prevention programmes. However, this non-monotonic behaviour disappears if the prevention programmes are sufficiently effective (figure 3b).

In the case of an outbreak, our results demonstrate a much simpler optimal resource allocation strategy. In both transmission-reducing and recovery-improving cases, increasing the effectiveness of an intervention implies the need to allocate more resources to that intervention measure (figure 4). This indicates that allocating more resources towards intervention strategies such as symptom monitoring programmes, which were reported to be very effective in preventing diseases like Ebola and SARS [25], might prove to be a more fruitful strategy than investing in new healthcare facilities during future outbreaks. However, when treatment programmes are highly effective, since the proportion of susceptible individuals can only decrease over subsequent times, it is unlikely that the risk of new infections will increase. Hence, resources need not be diverted to prioritize prevention programmes in such scenarios.

The appropriate allocation of limited resources during the early days of an outbreak can reduce the disease burden. The large change in the relative increase in peak size in the case of more effective control strategies highlights the opportunity to reduce disease burden with the help of timely intervention (figure 5a,b). When intervention measures are less effective, any delay in implementation does not influence the optimal strategy. However, when the interventions are highly

effective, although there is a large increase in the peak size for too much delay, there can be a wider range of optimal strategies (figure 5c).

Determining the optimal strategy also requires taking into account the nature of the returns from investments in intervention measures. When both prevention and recovery programmes give increasing or constant returns to scale, it is always optimal to invest entire resources into either one of them. On the other hand, decreasing returns from one or both intervention programmes increases the possibility of an optimal resource-sharing strategy (figures 7 and 8). This indicates that when prevention programmes concern measures such as contact tracing, which gives decreasing returns [50], a fraction of the resources must also be invested in treatment programmes. These findings are comparable to earlier studies on HIV where the allocation strategy ‘all-or-nothing’ in cases of increasing and constant returns, and resource sharing in the case of decreasing returns to scale were found to be optimal [31,32,35]. Additionally, for certain effectiveness of interventions, decreasing returns may help achieve a stable disease-free state or initial decay of outbreak size, which may not be possible otherwise (figures 7 and 8). This is because decreasing returns to scale imply relatively lower transmission and higher recovery rates for the same investment compared with the other return types. On increasing effectiveness further, there is an increased freedom to choose an optimal strategy to drive the system beyond the $\mathcal{R}_0^c = 1$ or $S_0\mathcal{R}_0^{\text{out}} = 1$ line.

In summary, this study provides a comprehensive understanding of how the effectiveness of different control measures determines an optimal strategy for resource allocation. Despite our minimalistic approach, our findings provide fundamental insights into the resource allocation problem in cases of infectious disease spread. A key limitation of our study is the assumption that increasing the investment of resources in intervention programmes can alter the transmission and recovery rates instantaneously. However, in reality, this is probably not the case. Additionally, factors such as the number of doctors or the success of prevention programmes largely depend on societal conditions, which were ignored in this study. Further, while we took into account the different types of production functions to determine the optimal strategies, we did not consider functions that may have a decreasing returns to scale, followed by an increasing returns to scale, or vice versa [32,35]. Albeit we acknowledge that it is not possible to make recommendations on policy design using such a simple framework, our model provides a foundational basis upon which more specific disease models may be studied in the future. The results highlight the importance of more systematic and involved analyses of the trade-offs among different available strategies by policymakers, especially in developing countries.

Data accessibility. Detailed proofs are available in the electronic supplementary material. The Matlab code supporting the results presented in the paper is available in the GitHub (https://github.com/abhisheksena/Optimal_resource) [51] repository.

The data are provided in electronic supplementary material [52].

Authors' contributions. B.M.: formal analysis, methodology, software, writing—original draft, writing—review and editing; S.B.: conceptualization, methodology, supervision, writing—review and editing; A.S.: conceptualization, methodology, supervision, writing—review and editing; J.C.: conceptualization, supervision, writing—review and editing. S.B. and A.S. contributed equally to this study.

All authors gave final approval for publication and agreed to be held accountable for the work performed therein.

Conflict of interest declaration. We declare we have no competing interests.

Funding. B.M. is supported by Junior Research Fellowship from University Grants Commission (UGC), India. A.S. and S.B. would like to acknowledge Senior Research Fellowship from CSIR, India for funding them during the initial part of this work. A.S. is also partially funded by the Center of Advanced Systems Understanding (CASUS), which is financed by Germany's Federal Ministry of Education and Research (BMBF) and by the Saxon Ministry for

Science, Culture and Tourism (SMWK) with tax funds on the basis of the budget approved by the Saxon State Parliament. S.B. was supported by the Visiting Scientist fellowship at Indian Statistical Institute, Kolkata during a part of this work. S.B. would also like to acknowledge his present funding under the Marie Skłodowska-Curie grant agreement no. 101025056 for the project 'SpatialSAVE'.

Acknowledgements. The authors would like to thank the anonymous referees for their comments and suggestions which have greatly enriched the manuscript.

References

- Fraser C *et al.* 2009 Pandemic potential of a strain of influenza A (H1N1): early findings. *Science* **324**, 1557–1561. (doi:10.1126/science.1176062)
- Colizza V, Barrat A, Barthélemy M, Vespignani A. 2007 Predictability and epidemic pathways in global outbreaks of infectious diseases: the SARS case study. *BMC Med.* **5**, 1–13. (doi:10.1186/1741-7015-5-34)
- Hufnagel L, Brockmann D, Geisel T. 2004 Forecast and control of epidemics in a globalized world. *Proc. Natl Acad. Sci. USA* **101**, 15 124–15 129. (doi:10.1073/pnas.0308344101)
- Légrand J, Grais RF, Boelle PY, Valleron AJ, Flahault A. 2007 Understanding the dynamics of Ebola epidemics. *Epidemiol. Infect.* **135**, 610–621. (doi:10.1017/S0950268806007217)
- Zhang J *et al.* 2020 Changes in contact patterns shape the dynamics of the COVID-19 outbreak in China. *Science* **368**, 1481–1486. (doi:10.1126/science.abb8001)
- Mahase E. 2020 China coronavirus: WHO declares international emergency as death toll exceeds 200. *Br. Med. J.* **368**, m408. (doi: 10.1136/bmj.m408)
- Gubler DJ. 2002 Epidemic dengue/dengue hemorrhagic fever as a public health, social and economic problem in the 21st century. *Trends Microbiol.* **10**, 100–103. (doi:10.1016/S0966-842X(01)02288-0)
- McMahon DE, Peters GA, Ivers LC, Freeman EE. 2020 Global resource shortages during COVID-19: bad news for low-income countries. *PLoS Negl. Trop. Dis.* **14**, e0008412. (doi:10.1371/journal.pntd.0008412)
- Oshitani H, Kamigaki T, Suzuki A. 2008 Major issues and challenges of influenza pandemic preparedness in developing countries. *Emerg. Infect. Dis.* **14**, 875–880. (doi:10.3201/eid1406.070839)
- Hopman J, Allegranzi B, Mehtar S. 2020 Managing COVID-19 in low- and middle-income countries. *Jama* **323**, 1549–1550. (doi:10.1001/jama.2020.4169)
- Gostin LO. 2014 Ebola: towards an international health systems fund. *Lancet* **384**, e49–e51. (doi:10.1016/S0140-6736(14)61345-3)
- Gostin LO, Friedman EA. 2015 A retrospective and prospective analysis of the west African Ebola virus disease epidemic: robust national health systems at the foundation and an empowered WHO at the apex. *Lancet* **385**, 1902–1909. (doi:10.1016/S0140-6736(15)60644-4)
- Bong CL, Brasher C, Chikumba E, McDougall R, Mellin-Olsen J, Enright A. 2020 The COVID-19 pandemic: effects on low- and middle-income countries. *Anesth. Analg.* **131**, 86–92. (doi:10.1213/ANE.0000000000004846)
- WHO. 2005 *WHO checklist for influenza pandemic preparedness planning*. See <https://apps.who.int/iris/handle/10665/68980>.
- WHO. 2020 *Coronavirus disease 2019 (COVID-19): situation report, 73*. See <https://apps.who.int/iris/handle/10665/331686>.
- Benson CA, Brooks JT, Holmes KK, Kaplan JE, Masur H, Pau A. 2009 Guidelines for prevention and treatment opportunistic infections in HIV-infected adults and adolescents; recommendations from CDC, the National Institutes of Health, and the HIV Medicine Association/Infectious Diseases Society of America.
- Siegel JD, Rhinehart E, Jackson M, Chiarello L. 2007 2007 guideline for isolation precautions: preventing transmission of infectious agents in health care settings. *Am. J. Infect. Control* **35**, S65–S164. (doi:10.1016/j.ajic.2007.10.007)
- Adhikari SP *et al.* 2020 Epidemiology, causes, clinical manifestation and diagnosis, prevention and control of coronavirus disease (COVID-19) during the early outbreak period: a scoping review. *Infect. Dis. Poverty* **9**, 1–12. (doi:10.1186/s40249-020-00646-x)
- Angulo MT, Castaños F, Moreno-Morton R, Velasco-Hernández JX, Moreno JA. 2021 A simple criterion to design optimal non-pharmaceutical interventions for mitigating epidemic outbreaks. *J. R. Soc. Interface* **18**, 20200803. (doi:10.1098/rsif.2020.0803)
- Ngonghala CN, Iboi E, Eikenberry S, Scotch M, MacIntyre CR, Bonds MH, Gumel AB. 2020 Mathematical assessment of the impact of non-pharmaceutical interventions on curtailing the 2019 novel Coronavirus. *Math. Biosci.* **325**, 108364. (doi:10.1016/j.mbs.2020.108364)
- Farmer P. 2001 The major infectious diseases in the world—to treat or not to treat? *N. Engl. J. Med.* **345**, 208–210. (doi:10.1056/NEJM200107193450310)
- Mosadeghrad AM. 2014 Factors influencing healthcare service quality. *Int. J. Health Policy Manage.* **3**, 77–89. (doi:10.15171/ijhpm.2014.65)
- Emanuel EJ *et al.* 2020 Fair allocation of scarce medical resources in the time of COVID-19. *N. Engl. J. Med.* **382**, 2049–2055. (doi:10.1056/NEJMsb2005114)
- Sacchetto D, Raviolo M, Beltrando C, Tommasoni N. 2020 COVID-19 surge capacity solutions: our experience of converting a concert hall into a temporary hospital for mild and moderate COVID-19 patients. *Disaster Med. Public Health Prep.* **382**, 2049–2055. (doi:10.1017/dmp.2020.412)
- Peak CM, Childs LM, Grad YH, Buckee CO. 2017 Comparing nonpharmaceutical interventions for containing emerging epidemics. *Proc. Natl Acad. Sci. USA* **114**, 4023–4028. (doi:10.1073/pnas.1616438114)
- Zhang R, Li Y, Zhang AL, Wang Y, Molina MJ. 2020 Identifying airborne transmission as the dominant route for the spread of COVID-19. *Proc. Natl Acad. Sci. USA* **117**, 14 857–14 863. (doi:10.1073/pnas.2009637117)
- Beigel JH *et al.* 2020 Remdesivir for the treatment of COVID-19. *N. Engl. J. Med.* **383**, 1813–1826. (doi:10.1056/NEJMoa2007764)
- RECOVERY Collaborative Group. 2020 Effect of hydroxychloroquine in hospitalized patients with COVID-19. *N. Engl. J. Med.* **383**, 2030–2040. (doi:10.1056/NEJMoa2022926)
- Brandeau ML, Zaric GS, De Angelis V. 2005 Improved allocation of HIV prevention resources: using information about prevention program production functions. *Health Care Manage. Sci.* **8**, 19–28. (doi:10.1007/s10729-005-5213-6)
- Medlock J, Galvani AP. 2009 Optimizing influenza vaccine distribution. *Science* **325**, 1705–1708. (doi:10.1126/science.1175570)
- Alistar SS, Long EF, Brandeau ML, Beck EJ. 2014 HIV epidemic control—a model for optimal allocation of prevention and treatment resources. *Health Care Manage. Sci.* **17**, 162–181. (doi:10.1007/s10729-013-9240-4)
- Brandeau ML, Zaric GS. 2009 Optimal investment in HIV prevention programs: more is not always better. *Health Care Manage. Sci.* **12**, 27–37. (doi:10.1007/s10729-008-9074-7)
- Hansen E, Day T. 2011 Optimal control of epidemics with limited resources. *J. Math. Biol.* **62**, 423–451. (doi:10.1007/s00285-010-0341-0)
- Worby CJ, Chang HH. 2020 Face mask use in the general population and optimal resource allocation during the COVID-19 pandemic. *Nat. Commun.* **11**, 1–9. (doi:10.1038/s41467-020-17922-x)
- Brandeau ML, Zaric GS, Richter A. 2003 Resource allocation for control of infectious diseases in multiple independent populations: beyond cost-

- effectiveness analysis. *J. Health Econ.* **22**, 575–598. (doi:10.1016/S0167-6296(03)00043-2)
36. Senapati A, Sardar T, Ganguly KS, Ganguly KS, Chattopadhyay AK, Chattopadhyay J. 2019 Impact of adult mosquito control on dengue prevalence in a multi-patch setting: a case study in Kolkata (2014–2015). *J. Theor. Biol.* **478**, 139–152. (doi:10.1016/j.jtbi.2019.06.021)
37. Calabrese JM, Demers J. 2022 How optimal allocation of limited testing capacity changes epidemic dynamics. *J. Theor. Biol.* **538**, 111017. (doi:10.1016/j.jtbi.2022.111017)
38. Ghosh S, Senapati A, Chattopadhyay J, Hens C, Ghosh D. 2021 Optimal test-kit-based intervention strategy of epidemic spreading in heterogeneous complex networks. *Chaos* **31**, 071101. (doi:10.1063/5.0053262)
39. Bolzoni L, Bonacini E, Della Marca R, Groppi M. 2019 Optimal control of epidemic size and duration with limited resources. *Math. Biosci.* **315**, 108232. (doi:10.1016/j.mbs.2019.108232)
40. Anderson RM, May RM. 1992 *Infectious diseases of humans: dynamics and control*. Oxford, UK: Oxford University Press.
41. Breda D, Diekmann O, De Graaf W, Pugliese A, Vermiglio R. 2012 On the formulation of epidemic models (an appraisal of Kermack and McKendrick). *J. Biol. Dyn.* **6**, 103–117. (doi:10.1080/17513758.2012.716454)
42. Kaplan EH. 1995 Economic analysis of needle exchange. *AIDS* **9**, 1113–1120. (doi:10.1097/00002030-199510000-00001)
43. Zaric GS, Brandeau ML. 2001 Optimal investment in a portfolio of HIV prevention programs. *Med. Decis. Making* **21**, 391–408. (doi:10.1177/0272989X0102100506)
44. Lima VD, Johnston K, Hogg RS, Levy AR, Harrigan PR, Anema A, Montaner JS. 2008 Expanded access to highly active antiretroviral therapy: a potentially powerful strategy to curb the growth of the HIV epidemic. *J. Infect. Dis.* **198**, 59–67. (doi:10.1086/588673)
45. Zaric GS, Barnett PG, Brandeau ML. 2000 HIV transmission and the cost-effectiveness of methadone maintenance. *Am. J. Public Health* **90**, 1100–1111. (doi:10.2105/AJPH.90.7.1100)
46. Zaric GS, Brandeau ML, Barnett PG. 2000 Methadone maintenance and HIV prevention: a cost-effectiveness analysis. *Manage. Sci.* **46**, 1013–1031. (doi:10.1287/mnsc.46.8.1013.12025)
47. Keeling MJ, Rohani P. 2011 *Modeling infectious diseases in humans and animals*. Princeton, NJ: Princeton University Press.
48. Martcheva M. 2015 *An introduction to mathematical epidemiology*, vol. 61. New York, NY: Springer.
49. Deka A, Bhattacharyya S. 2019 Game dynamic model of optimal budget allocation under individual vaccination choice. *J. Theor. Biol.* **470**, 108–118. (doi:10.1016/j.jtbi.2019.03.014)
50. Armbruster B, Brandeau ML. 2007 Contact tracing to control infectious disease: when enough is enough. *Health Care Manage. Sci.* **10**, 341–355. (doi:10.1007/s10729-007-9027-6)
51. Maity B, Banerjee S, Senapati A, Chattopadhyay J. 2023 Quantifying optimal resource allocation strategies for controlling epidemics. *GitHub*. https://github.com/abhisheksena/Optimal_resource.
52. Maity B, Banerjee S, Senapati A, Chattopadhyay J. 2023 Quantifying optimal resource allocation strategies for controlling epidemics. *Figshare*. (doi:10.6084/m9.figshare.c.6631156)